Performance Evaluation 66 (2009) 742–753

Contents lists available at ScienceDirect

Performance Evaluation

journal homepage: www.elsevier.com/locate/peva

Capacity fades analysis of MIMO Rician channels in mobile ad hoc networks☆,☆☆

Li-Chun Wang [a], Wei-Cheng Liu [a,*], Yun-Huai Cheng [b]

[a] Department of Communications Engineering, National Chun Cheng University, 168 University Road, Min-Hsiung, Chia-Yi, 62102, Taiwan

[b] Foxconn International Holdings, Co., Ltd., 10F., No.19-2, Sanchong Road, Nangang District, Taipei City 11501, Taiwan

ARTICLE INFO

Article history:
Received 2 December 2008
Received in revised form 5 July 2009
Accepted 6 August 2009
Available online 12 August 2009

Keywords:
Average capacity fading duration
Level crossing rate
Mobile-to-mobile MIMO channel model
Rician fading
Sum-of-sinusoids method

ABSTRACT

Multiple-input multiple-output (MIMO) mobile ad hoc networks have been receiving increased attention in both commercial and military applications. Just as in cellular networks, MIMO technologies can benefit ad hoc networks by providing the diversity and capacity advantages as well as the spatial degree of freedom in designing the media access control (MAC) protocol. However, one fundamental issue of MIMO mobile ad hoc networks is how to accurately model the impact of spatial/temporal channel correlation in the mobile-to-mobile communications environment. In such a channel, line-of-sight (LOS) components and different scattering environments will affect both ergodic capacity and average capacity fading duration of the MIMO system. In this paper, based on the double-ring scattering model with LOS components we suggest a sum-of-sinusoids MIMO mobile-to-mobile channel simulation method, which can characterize the spatial/temporal channel correlation and Rician fading effect. Our numerical results show the ergodicity of our proposed channel model, correctness of the analytical channel correlation, effect of spatial correlation on channel capacity, impact of the number of antennas and scatterers on capacity, capacity distribution, and level crossing rate (LCR) and average fading duration (AFD) of MIMO Rician channel capacity. We also show the impacts of Rician factor K on channel capacity, probability density function (PDF), LCR, and AFD.

1. Introduction

Multiple-input multiple-output (MIMO) antenna technique has recently emerged as one of the most significant breakthroughs in communications. The fourth generation (4G) cellular system [1] and the next generation high-speed IEEE 802.11n [2] wireless local area network (WLAN) all adopt the MIMO technique to deliver capacity and diversity gains.

Meanwhile, another communication paradigm – ad hoc networks – has become an important alternative for next generation wireless systems. In contrast to conventional cellular systems with a master–slave relation between the base station and mobile users, nodes in ad hoc networks adopt peer-to-peer communications. Specifically, this communication is supported by direct connection or multiple hop relays without fixed wireless infrastructure. Ad hoc networks have been enabled in many standards such as Bluetooth and IEEE 802.11 WLAN. Ad hoc networking is considered the key enabling technique of many future wireless systems, such as wireless mesh networks [3] and cognitive radio [4].

Unlike conventional mobile-to-fixed base station systems that have been benefited from the MIMO technique, how and to what extent the ad hoc networks can benefit from the MIMO technique is still an open research area. One fundamental

☆ This work was supported jointly by the National Science Council and the Program of Promoting Excellence of University of Ministry of Education, Taiwan under the contracts EX91-E-FA06-4-4, NSC93-2213-E-009-097, and NSC93-2219-E-009-012.

☆☆ Part of this work has been published in IEEE Vehicular Technology Conference Fall, Dallas, Sep., 2005.

* Corresponding author.
E-mail addresses: lichun@g2.nctu.edu.tw (L.-C. Wang), weichengliu@hotmail.com (W.-C. Liu), yunhuai.cheng@gmail.com (Y.-H. Cheng).

0166-5316/$ – see front matter © 2009 Elsevier B.V. All rights reserved.
doi:10.1016/j.peva.2009.08.006

issue is how to accurately model the impact of spatial/temporal correlation on MIMO capacity from the viewpoint of the mobile-to-mobile communications. Scattering model and the line-of-sight (LOS) components are two important factors that need to be considered. First, in a mobile-to-mobile environment, the antenna heights of both the transmitter and the receiver are lower than the surrounding objects. Thus, the signal in a mobile-to-mobile environment will experience a richer scattering effect than in a mobile-to-base environment [5–7]. Second, LOS components may more likely exist in a short-distance mobile-to-mobile application than in a long-distance mobile-to-base environment. In [8], the distribution of the Rician K factor was modeled as lognormal, with the median as a function of distance: $K \propto (\text{distance})^{-0.5}$. Implicitly, the K factor increases as the distance decreases. Thus, the Rician fading effect cannot be neglected in a short-distance mobile-to-mobile communication environment.

In the literature, some MIMO channel models have been reported. In [9], the authors proposed a MIMO channel model, considering clusters effect, Doppler frequency, mean angular spread (AS), mean angle-of-arrival (AoA), and angle-of-departure (AoD) of each cluster and corresponding taps. The WINNER channel model described in [10] is a geometry-based stochastic MIMO model specifying pathloss, delay spread, AoD spread (ASD), AoA spread (ASA), shadowing fading, Rician K factor, delay distribution, AoD and AoA distributions, number of clusters, number of rays per cluster, cluster ASD and ASA, per cluster shadowing, and correlation distance. The 3GPP spatial channel model (SCM) [11] consists of number of paths, number of sub-paths per-path, AS at base station (BS), per-path AS at BS, BS per-path AoD distribution, mean AS at mobile station (MS), per-path AS at MS, MS per-path AoA distribution, delay spread, mean total RMS delay spread, distribution for path delays, lognormal shadowing standard deviation, and pathloss model.

Some important references in MIMO mobile-to-mobile (M2M) channel models are as follows. In [12,13], the authors proposed a MIMO M2M channel model derived from the geometrical two-ring model. In [14], the authors proposed a theoretical model for MIMO M2M Rayleigh fading channel. In [15], the authors proposed two new sum-of-sinusoids (SoS) based simulation models for MIMO M2M Rayleigh fading channels. In [16], the authors proposed a three-dimensional (3D) MIMO M2M channel model. In [17], the authors proposed a 3D geometrical propagation model for wideband MIMO M2M communications. In [18], the authors derived a MIMO M2M channel model from a geometric street scattering model. In [19], the author investigated the statistical properties of narrowband MIMO M2M wireless fading channels in non-isotropic scattering environments based on the elliptical-ring model. In [20], the authors proposed a single- and double-bounced two-ring parametric reference model for MIMO M2M Rician fading channels. In [21], the authors proposed a 3D reference model for MIMO M2M multipath fading channels and derived the space–time correlation on the outage capacity. In [22], the authors proposed a space–time–frequency (STF) non-isotropic MIMO M2M multicarrier Rician fading channel model. In [23], the authors proposed a generic geometrical-based MIMO M2M channel model. In [24], the authors derived a wideband multiple-cluster MIMO M2M channel model based on their results in [18]. In [25], the authors proposed a novel isotropic scatter distribution wideband MIMO M2M fading channel model. In [26], the authors presented a vehicle-to-vehicle (VTV) MIMO channel model based on measurements. Compared with above related works, we provide not only a MIMO M2M channel model but also analysis of the capacity fades.

The comparisons between some previous works and our work are listed as follows. In [27], the authors described the capacity behavior of outdoor MIMO channels as a function of scattering radii, antenna beamwidths, antenna spacing, and the distance between the transmit and receive arrays. In our paper, we only consider the antenna spacing for simplicity, but we consider Rician fading, LCR, AFD, and the impact of the number of scatterers. In [28], the author derived a general model for the MIMO wireless channel which considered the interdependency of directions-of-arrival and directions-of-departure, angle dispersion by far clusters, and rank reduction of the transfer function matrix. Our proposed MIMO channel is an extension of Jake's model, which can help channel simulation by only considering the channel correlation in both spatial and time domain. In [29], the authors derived the MIMO capacity, LCR, and AFD considering the impact of spatial/temporal channel correlation using one-ring model. In our paper, the two-ring scattering model is adopted to capture the channel characteristics of mobile-to-mobile communications. Further, we consider the impact of the Rician K factor and the number of scatterers on the total channel capacity, both of which are not considered in [29]. In [30], the authors proposed a single-bounce two-ring statistical model for the time-varying MIMO flat Rayleigh fading channels and derived the spatial–temporal correlations, LCR and AFD of the fading envelope, and the instantaneous mutual information (IMI). However, they did not consider the impact of Rician K factor, number of scatterers, and the antenna separation. In our paper, LCR and AFD are used to study the temporal behavior of the MIMO capacity. In [31], the authors investigated the effects of fading correlations in MIMO systems using the one-ring model. In our paper, we consider the general two-ring model and derive the LCR, AFD, and an upper bound for the average channel capacity. In [32], the author presented the narrowband one-ring and two-ring models but did not consider LOS components. In our channel model, we include the LOS components and consider the impact of Rician K factor on channel capacity, LCR, and AFD. In [33], the authors analyzed the symbol error probability (SEP), the effective fading figure (EFF), and the capacity at low signal-to-noise ratio (SNR) for double scattering MIMO channels. Compared with our paper, they did not consider the two-ring model with LOS components, LCR, AFD, impacts of number of antennas, number of scatterers, and Rician K factor on channel capacity.

The objective of this paper is two-fold. First, we aim to develop a simple sum-of-sinusoids MIMO channel simulation method that can characterize the spatial/temporal correlation and Rician fading effect. The sum-of-sinusoids channel simulation method, or 'Jake's model', has been widely used to evaluate the performance of conventional single-input single-output (SISO) mobile systems [34–36]. Jake's model can capture the time behavior of a mobile-to-base channel. Recently, in [6], a mobile-to-mobile MIMO channel simulator was developed to incorporate the spatial correlation in a Rayleigh fading

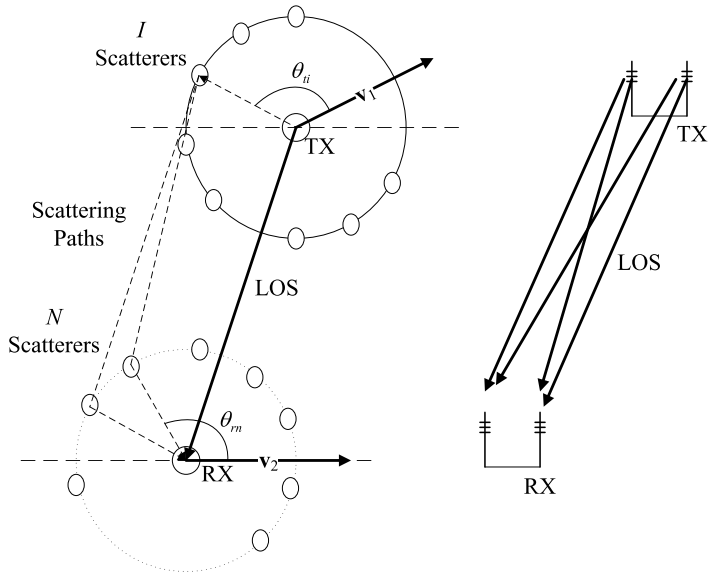

Fig. 1. Double-ring scattering model with LOS components.

environment. We will further incorporate the Rician fading effect in the mobile-to-mobile MIMO channel simulator based on a double-ring scattering model with LOS components (described in Section 3). The second objective of this paper is to research the capacity of the mobile-to-mobile MIMO Rician fading channel. To this end, we will derive the upper bound of the ergodic capacity of the mobile-to-mobile MIMO Rician channel. The MIMO capacity bound can be used to confirm the accuracy of the proposed sum-of-sinusoids simulation method and explore the impact of spatial correlation. Further, we evaluate the level crossing rate (LCR) and average fading duration (AFD) of the MIMO mobile-to-mobile Rician channel. The LCR and AFD of MIMO capacity was researched in [37,38], but not in a mobile-to-mobile and not in a Rician fading channel, either. We will relate the LCR and capacity fading of MIMO mobile-to-mobile systems with the Rician K factor.

The rest of this paper is organized as follows. Section 2 describes the scattering model for the mobile-to-mobile communications system. In Section 3, we introduce the sum-of-sinusoids MIMO Rician fading simulator. In Section 4, we evaluate the ergodic capacity and capacity fading duration of the MIMO Rician fading channel based on the proposed simulation method. In Section 5, we show numerical results to elaborate the impacts of the Rician K factor, spatial correlation, and temporal correlation on the MIMO mobile-to-mobile systems. We give our concluding remarks in Section 6.

2. Mobile-to-mobile scattering model

In this section, we introduce the double-ring scattering model with LOS components [7]. This model can be used to capture the scattering effect and the LOS effect in a mobile-to-mobile environment as shown in Fig. 1. In the figure, the transmitter and the receiver moving at a speed of $\mathbf{v}_1$ and $\mathbf{v}_2$, are surrounded by I and N scatterers, respectively. The AoD between vector $\mathbf{v}_1$ and scattering paths, denoted by θ_{ti} $(i = 1, 2, \ldots, I)$ and θ_{rn} $(n = 1, 2, \ldots, N)$, are the angles of arrival between vector $\mathbf{v}_2$ and the scattering paths. We assume that θ_{ti} and θ_{rn} are independent and uniformly distributed over $[-\pi, \pi)$. Note that there exist LOS components between the transmitter TX and the receiver RX, where both TX and RX are equipped with multiple antennas. Furthermore, we assume an isotropic scattering environment throughout this paper. Transmission delays of the scattered paths are not considered in our scheme.

Consider that the multiple antennas are separated by a distance d. Antennas are omnidirectional and are arranged in a line which is perpendicular to the moving direction of TX and RX. In the case where transmission distance from the scatterers to the receive antenna is much longer than d, then the AoA from the nth scatterer to each receive antenna will be about the same. Thus, for the case with two receive antennas, the transmission distance from the nth scatterer to the second receive antenna is $d \cos \theta_{rn}$ longer than that to the first receive antenna.

Our model is suitable for an outdoor environment, mobile-to-mobile ad hoc network. For example, a vehicular ad hoc network (VANET) [39] is a form of mobile ad hoc network, which can adopt our scenario and results. Furthermore, our model considers a LOS component, which applies to the case of short-distance communications.

3. Sum-of-sinusoids simulator for MIMO Rician fading channels

3.1. LOS components model

To begin with, we discuss the approach to model the LOS components between each pair of moving transmit and receive antennas. For simplicity, we first consider the single antenna case. Referring to Fig. 2, let the transmitter TX move at a speed

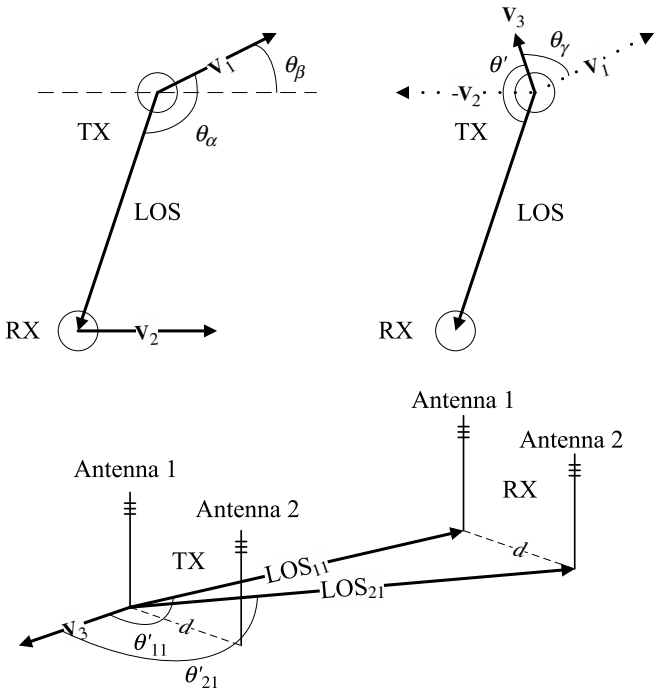

Fig. 2. LOS component model for moving transmitter TX and receiver RX of which velocity vectors are $\mathbf{v}_1$ and $\mathbf{v}_2$ with a relative angle of θ_β, respectively.

of $\mathbf{v}_1$ toward the direction of the angle θ_β relative to the direction of velocity $\mathbf{v}_2$ of receiver RX, where θ_α is the angle between $\mathbf{v}_1$ and the transmission direction of the LOS components. Using the concept of relative motion [40], let the velocity of RX be zero and denote $\mathbf{v}_3$ the relative velocity from TX to RX, as shown in Fig. 2. In the figure, θ' is the angle between $\mathbf{v}_3$ and LOS component. The relative velocity $\mathbf{v}_3$ can be derived as follows:

$$|\mathbf{v}_3| = \sqrt{(|\mathbf{v}_1|\cos\theta_\beta - |\mathbf{v}_2|)^2 + (|\mathbf{v}_1|\sin\theta_\beta)^2}, \tag{1}$$

$$\theta' = 2\pi - \theta_\alpha - \theta_\gamma, \tag{2}$$

and

$$\theta_\gamma = \cos^{-1}\left(\frac{|\mathbf{v}_1|^2 + |\mathbf{v}_3|^2 - |\mathbf{v}_2|^2}{2|\mathbf{v}_1||\mathbf{v}_3|}\right), \tag{3}$$

where $|\mathbf{v}|$ is the length of a vector $\mathbf{v}$, θ_γ is the angle between velocity vectors $\mathbf{v}_3$ and $\mathbf{v}_1$. Thus the LOS component can be expressed as

$$\text{LOS} = \sqrt{K}\exp[j(2\pi f_c t - 2\pi f_3 t\cos\theta')], \tag{4}$$

where the Rician K factor is defined as the ratio of the specular power to scattering power [36], f_c is the carrier frequency, $f_3 = |\mathbf{v}_3|/\lambda$ is the relative maximum Doppler frequency between TX and RX, and λ is the wavelength.

Now, we consider the scenario with multiple antennas. Define H_{ml} as the complex channel gain between the lth transmit antenna and mth receive antenna. From Fig. 2, the LOS components for H_{11} and H_{21} can be respectively expressed as

$$\text{LOS}_{11} = \sqrt{K_{11}}\exp[j(2\pi f_c t - 2\pi f_3 t\cos\theta'_{11})] \tag{5}$$

and

$$\text{LOS}_{21} = \sqrt{K_{21}}\exp[j(2\pi f_c t - 2\pi f_3 t\cos\theta'_{21})], \tag{6}$$

where K_{ml} is the Rician factor defined as the ratio of specular power to the scattering power of the channel H_{ml} [41]; θ'_{11} and θ'_{21} are the angles between the LOS components LOS_{11} and LOS_{21} to the velocity vector $\mathbf{v}_3$, respectively. Assume that the transmission distance between the two mobiles is much longer than the antenna separation d. Then, the angles θ'_{11} and θ'_{21} are about the same. Likewise, $\theta'_{21} = \theta'_{22} = \theta'_{11} = \theta'_{12}$. To ease notation for all m and l, let

$$\rho = 2\pi f_c t - 2\pi f_3 t\cos\theta'_{ml}. \tag{7}$$

3.2. Sum-of-sinusoids simulation method

Based on the double-ring scattering model and the LOS components model which was proposed in [42], we suggest the sum-of-sinusoids simulation method for a mobile-to-mobile MIMO channel model with LOS components. Consider

narrowband signals in a flat Rician fading channel. The MIMO channel is expressed as an $M \times L$ matrix $\mathbf{H}$, where M and L are the numbers of antennas at the receiver and transmitter, respectively. H_{ml} is the element of the mth row and lth column. With this notation, we have

$$H_{11} = \frac{1}{\sqrt{1+K_{11}}}\left[\frac{1}{\sqrt{IN}}\sum_{n=1}^{N}\sum_{i=1}^{I}A_{in}\exp(j\phi_{in}) + \sqrt{K_{11}}\exp(j\rho)\right], \tag{8}$$

where

$$\phi_{in} = 2\pi f_c t - 2\pi f_2 t\cos\theta_{rn} - 2\pi f_1 t\cos\theta_{ti}, \tag{9}$$

A_{in} and ϕ_{in} are the amplitude and phase of the inth scattering path, respectively, $f_1 = |\mathbf{v}_1|/\lambda$ and $f_2 = |\mathbf{v}_2|/\lambda$ are the maximum Doppler frequencies resulted from the motion of TX and RX, respectively, I and N are the numbers of the scatterers around TX and RX, respectively.

For H_{21}, we further consider the added transmission delay because of the antenna separation d. Thus, it follows that

$$H_{21} = \frac{1}{\sqrt{1+K_{21}}}\left[\frac{1}{\sqrt{IN}}\sum_{n=1}^{N}\sum_{i=1}^{I}A_{in}\exp(j\phi_{in} + j\beta d(2-1)\cos\theta_{rn}) + \sqrt{K_{21}}\exp(j\rho)\right], \tag{10}$$

where $\beta = 2\pi/\lambda$ is the wave number. Thus, the general form of the channel H_{ml} can be computed by

$$H_{ml} = \frac{1}{\sqrt{1+K_{ml}}}\left[\frac{1}{\sqrt{IN}}\sum_{n=1}^{N}\sum_{i=1}^{I}A_{in}\exp(j\phi_{in} + j\beta d(m-1)\cos\theta_{rn} + j\beta d(l-1)\cos\theta_{ti}) + \sqrt{K_{ml}}\exp(j\rho)\right], \tag{11}$$

for every $m = 1, 2, \ldots, M$ and $l = 1, 2, \ldots, L$.

4. Capacity evaluation

Consider an $M \times L$ MIMO channel matrix, and assume that the knowledge of a frequency flat faded signal can be known perfectly at the receiver. Let $\mathbf{n}$ be an $M \times 1$ zero mean complex AWGN vector, of which the covariance matrix is equal to $\sigma^2\mathbf{I}_M$, where $\mathbf{I}_M$ stands for an $M \times M$ identity matrix. The $M \times 1$ received signal vector $\mathbf{y}$ can be expressed as [43]

$$\mathbf{y} = \mathbf{H}\mathbf{x} + \mathbf{n}, \tag{12}$$

where $\mathbf{x}$ is an $L \times 1$ transmitted signal vector.

4.1. Ergodic capacity

The instantaneous capacity of an MIMO channel can be written as [44–46]

$$c(t) = \begin{cases} \log_2\left[\det\left(\mathbf{I}_M + \dfrac{\mathrm{SNR}}{L}\cdot\mathbf{H}\mathbf{H}^{\dagger}\right)\right] & \text{if } M < L, \\ \log_2\left[\det\left(\mathbf{I}_L + \dfrac{\mathrm{SNR}}{L}\cdot\mathbf{H}^{\dagger}\mathbf{H}\right)\right] & \text{if } M \geq L, \end{cases} \tag{13}$$

where $\dagger$ denotes transpose conjugate.

In this part, we derive the channel correlation and find its channel capacity. The channel correlation between H_{11} and H_{21} is [6]

$$\Delta_{11,21} = E[H_{11}H_{21}^{*}], \tag{14}$$

where $*$ is the complex conjugate. Assume that the number of scatterers around the transmitter and receiver equals N; A_{in} is a zero mean unit variance normal random variable because of the central limit theorem for many scatterers; θ_{ti} and θ_{rn} are uniform random variables. All the above random variables are mutually independent. Then, we have

$$\Delta_{11,21} = \frac{J_0(\beta d) + \sqrt{K_{11}}\sqrt{K_{21}}}{\sqrt{1+K_{11}}\sqrt{1+K_{21}}}. \tag{15}$$

The general form of the channel correlation between H_{ml} and H_{pq} should be expressed as

$$\Delta_{ml,pq} = \frac{J_0(\beta d(m-p))J_0(\beta d(l-q)) + \sqrt{K_{ml}}\sqrt{K_{pq}}}{\sqrt{1+K_{ml}}\sqrt{1+K_{pq}}}, \tag{16}$$

where $J_0(\cdot)$ is the zeroth-order Bessel function of the first kind.

From (13), the average capacity of the MIMO channel can be expressed as

$$C_E = E\left[\log_2\left(\det\left(\mathbf{I}_M + \frac{\mathrm{SNR}}{L}\cdot\mathbf{H}\mathbf{H}^\dagger\right)\right)\right]. \tag{17}$$

By using Jensen's inequality, we conclude that the average capacity is bounded by

$$C_E \le \log_2\left(\det\left(\mathbf{I}_M + \frac{\mathrm{SNR}}{L}\cdot E[\mathbf{H}\mathbf{H}^\dagger]\right)\right). \tag{18}$$

Let $\mathbf{R}$ denote the correlation channel matrix $E[\mathbf{H}\mathbf{H}^\dagger]$, where

$$R_{ij} = \sum_{v=1}^{L} E[H_{iv}H_{jv}^*] = \sum_{v=1}^{L} \frac{J_0(\beta d(i-j)) + \sqrt{K_{iv}}\sqrt{K_{jv}}}{\sqrt{1+K_{iv}}\sqrt{1+K_{jv}}}. \tag{19}$$

Thus, we can derive the entire correlation channel matrix $\mathbf{R}$ and channel capacity from (19). Substituting $\mathbf{R}$ into (18), we can find an upper bound for the mobile-to-mobile MIMO channel capacity.

4.2. Level crossing rate and average fading duration

To examine the temporal behavior of the MIMO capacity, we first study the level crossing rate (LCR) and average fading duration (AFD). Denote L_ε and τ_ε the LCR across a specified level ε of the capacity $c(t)$, and the AFD below the level ε, respectively. Based on the definition of LCR [47], we have

$$L_\varepsilon = \int_0^\infty \dot{c}\, p_{c,\dot{c}}(\varepsilon, \dot{c})\mathrm{d}\dot{c} \tag{20}$$

where $\dot{c} \triangleq \frac{\mathrm{d}c(t)}{\mathrm{d}t}$ is the derivative of the channel capacity with respect to time t; $p_{c,\dot{c}}(c, \dot{c})$ is the joint probability density function (PDF) of the channel capacity and its derivative. Obviously, how to obtain the joint PDF $p_{c,\dot{c}}(c, \dot{c})$ is the key issue to calculate L_ε. From [48,37,49], we know that the capacity distribution for MIMO systems in the independent Rayleigh fading channel can be estimated by Gaussian distribution. Whether the Gaussian approximation of the MIMO capacity is accurate for the Rician fading channel is less well known. Further, it is worthwhile examining if a Gaussian sequence can match the temporally correlated sequence of MIMO capacity in a Rician fading channel. To this end, we first hypothesize that the capacity distribution of the mobile-to-mobile MIMO Rician channel is Gaussian. In Section 5, we will perform simulations based on the proposed sum-of-sinusoids method to confirm this theory. If the MIMO capacity $c(t)$ in the mobile-to-mobile Rician fading channel is accurately estimated by a Gaussian process, the LCR problem can be solved by using Rice's formula of stochastic processes [34]. Specifically, we can have

$$L_\varepsilon = \frac{(-\ddot{\rho}_c(0))^{1/2}}{2\pi}\exp\left(-\frac{\varepsilon^2}{2}\right), \tag{21}$$

where $\rho_c(\tau)$ is the autocorrelation function of $c(t)$ and $-\ddot{\rho}_c(0) = \mathrm{var}\left(\frac{\mathrm{d}c(t)}{\mathrm{d}t}\right)\Big|_{t=0}$. Since the analytical formula of $\rho_c(\tau)$ is not available [50], we adopt a semi-analytical method. That is, we obtain $-\ddot{\rho}_c(0)$ from simulation data and then substitute it into (21). Once L_ε is known, it follows that

$$\tau_\varepsilon = \frac{F_c(\varepsilon)}{L_\varepsilon}, \tag{22}$$

where $F_c(\cdot)$ is the cumulative density function (CDF) of channel capacity $c(t)$. Note that $F_c(\cdot)$ can be obtained by pure simulation or the CDF of a Gaussian random variable with a mean and variance from the simulation data.

5. Numerical results

In our simulations, we randomly generate the mobile-to-mobile MIMO channel matrix $\mathbf{H}$ and calculate the channel capacity of $\mathbf{H}$ according to (17). The purposes of simulations are the following. First, we want to prove the ergodicity of our MIMO channel capacity model by examining time and ensemble averages. Second, we evaluate the capacity of MIMO Rician fading channel with different Doppler frequencies. Third, we vary the antenna separations and the Rician factors to explore the relationship between spatial channel correlation and channel capacity. Then, we vary the numbers of scatterers to inspect the scattering effect to the MIMO channel capacity. Finally, we compare the PDF of the channel capacity with Gaussian distribution to verify the correctness of the hypothesis used in Section 4. We will present the LCR and AFD of MIMO capacity for various Rician factor and number of antennas.

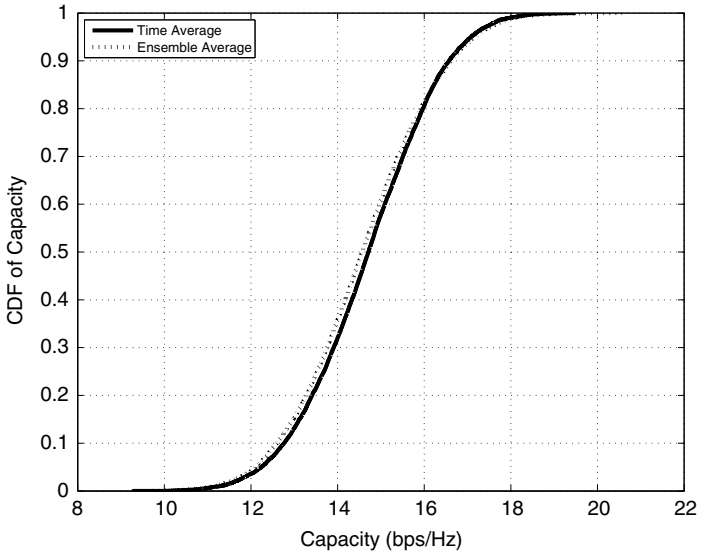

Fig. 3. The time and the ensemble average capacity CDF of a 3×3 MIMO channel when $K = 3$, SNR $= 20$ dB, and $d = \lambda/2$.

Table 1
The simulation parameters for Fig. 3.

Parameter	Value
Simulation time	10 s
Sampling rate	1000 Hz
Velocity of TX ($\mathbf{v}_1$)	100 m/s
Velocity of RX ($\mathbf{v}_2$)	10 m/s
Angle between $\mathbf{v}_1$ and LOS (θ_α)	$\pi/6$
Angle between $\mathbf{v}_1$ and $\mathbf{v}_2$ (θ_β)	$\pi/3$
Number of TX antennas	3
Number of RX antennas	3
Rician factor (K)	3
Number of scatterers around TX (I)	8
Number of scatterers around RX (N)	8
Carrier frequency (f_c)	10^9 Hz
Antenna separation	15 cm
SNR	20 dB

5.1. Ergodicity

Fig. 3 shows the capacity CDF of a time average and an ensemble average for a mobile-to-mobile Rician MIMO channel. The simulation parameters are listed in Table 1. From the figure, one can see that these two averages match quite well. This property implies that our channel model is ergodic.

5.2. Comparison of M2M and M2B channels

Fig. 4 shows the CDF of capacity of mobile-to-mobile (M2M) and mobile-to-base (M2B) channels for Rician factor $K = 1$ and 10. The other parameters are the same as in the previous figure. Compared with M2B channels, M2M has lower capacity. It conforms to our common sense that the system capacity is higher in a static environment more than that of mobile one. Increasing K will decrease the capacity, because as K increases, the LOS power increases and the scattering power decreases, the spatial correlation increases and the channel capacity decreases.

5.3. Channel correlation

To check the correctness of (16), we calculate the analytical and simulation values of the channel correlations of a 3×3 MIMO channel with SNR = 20 dB, $d = \frac{\lambda}{2}$, and $K = 4.77$ dB, which are listed in Table 2. We can see the analytical and simulation values are very close. Note that the analytical value for $\Delta_{ml,pq}$ in (16) is a real number. In Table 2, the simulation values have a small or zero imaginary part, which agrees with (16).

5.4. Capacity distribution

Fig. 5 shows the PDF of the 2×2 MIMO capacity in mobile-to-mobile Rician fading channels. The antenna distance $d = 2\lambda$. In the figure, we see that the PDF of the MIMO capacity in Rician fading channels can be approximated by Gaussian PDF. As

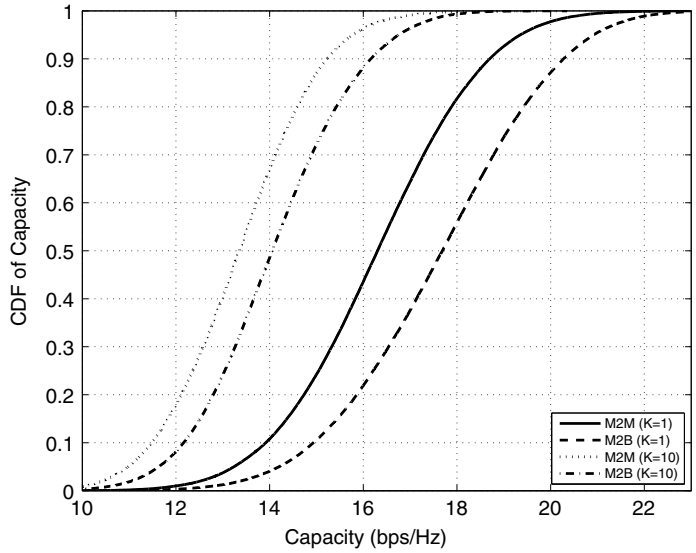

Fig. 4. The CDF of capacity of mobile-to-mobile (M2M) and mobile-to-base-station (M2B) channels for Rician factor $K = 1$ and 10.

Table 2
The simulation and analytical values of the channel correlation of a 3×3 MIMO channel.

	$\Delta_{11,21}$	$\Delta_{11,22}$	$\Delta_{11,23}$	$\Delta_{11,13}$	$\Delta_{11,11}$
Analysis	0.6739	0.7731	0.7332	0.8051	1
Simulation	$0.6751 + j0.0792$	$0.7676 - j0.0227$	$0.7360 - j0.0273$	$0.7966 - j0.0532$	1.0182

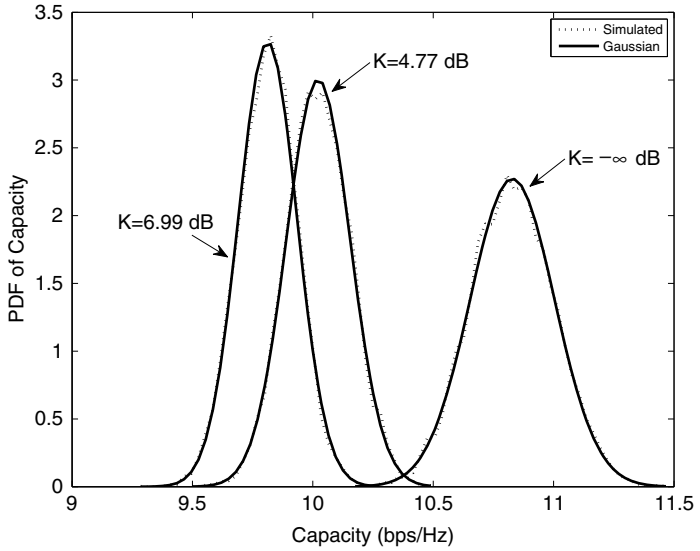

Fig. 5. Probability density functions of MIMO capacity in a mobile-to-mobile Rician fading channel.

the Rician factor K increases, the MIMO capacity decreases and varying capacity is also reduced. We also check the accuracy of Gaussian approximation for the MIMO capacity in a mobile-to-mobile Rician fading channel by changing different Doppler frequencies and reach the same conclusion.

5.5. LCR and AFD

Figs. 6 and 7 show the LCR and AFD of the MIMO capacity in a mobile-to-mobile Rician fading channel. The antenna distance $d = 2\lambda$. We confirm the accuracy of Gaussian approximation used in the proposed semi-analytical model by simulations. In Fig. 6, we find that the range of the capacity crossing level decreases when K increases. This is mainly because the capacity correlation is proportional to the extent of the LOS components. Also, the extent of the capacity variation decreases when K increases. In Fig. 7, we find that the rate of rising of the AFD will rapidly increase when Rician factor increases. This phenomenon comes from that the variance of the channel capacity decreasing as K increasing, as we noted in Fig. 5.

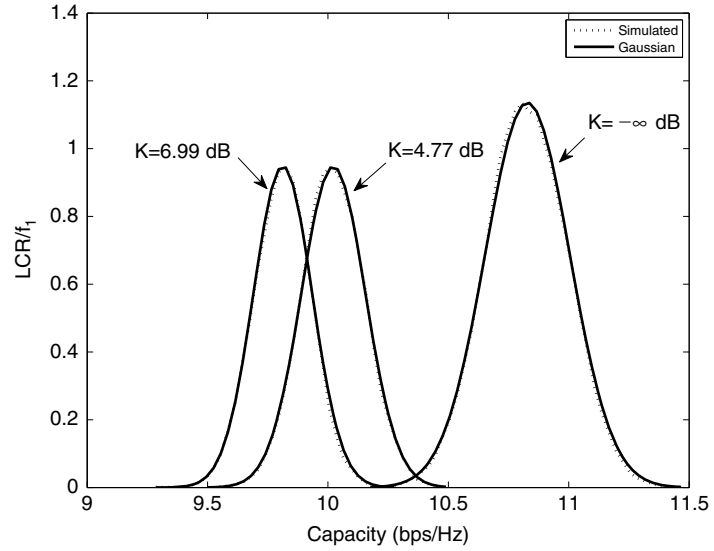

Fig. 6. Level crossing rate of the MIMO capacity in a mobile-to-mobile Rician fading channel. f_1 is the maximum Doppler frequency of the transmitter.

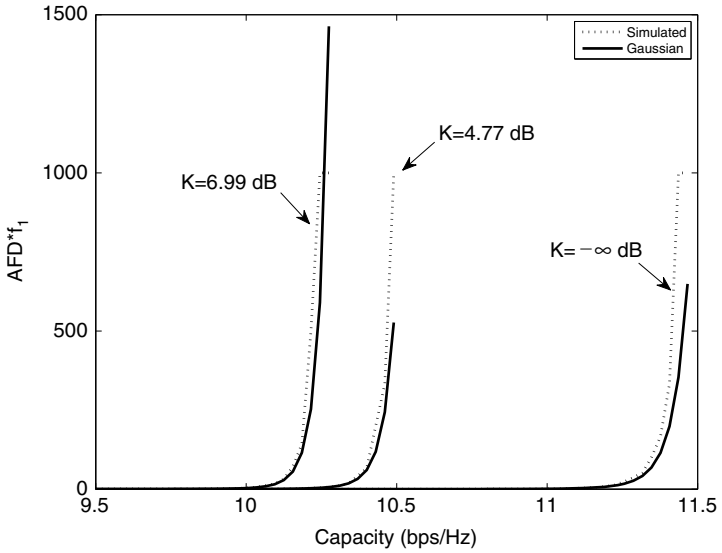

Fig. 7. Average fading duration of the MIMO capacity in a mobile-to-mobile Rician fading channel. f_1 is the maximum Doppler frequency of the transmitter.

5.6. Effect of spatial correlation

Fig. 8 shows the capacity of a 3×3 mobile-to-mobile MIMO channel for different Rician K factors and antenna separation d. The capacity obtained by the simulation is lower than its upper bound. In general, we find that the MIMO capacity grows with the increase of the antenna separations when $d \geq \frac{\lambda}{10}$, and it reaches the maximum when $d \geq \frac{\lambda}{2}$. We also find that the capacity vibrates when d becomes very large. This phenomenon results from the Bessel function in (16). Recall that the tail of the Bessel function is cosine vibration and its amplitude is exponentially decreased. For the fixed antenna separation, the other source of channel correlation is from the Rician factor. Based on (16), if the channel correlation arises, the capacity reduced at the same time. Therefore, the capacity with $K = 4.77$ dB shown in the figure is lower than that with $K = -\infty$ dB and $K = 0$ dB.

5.7. Impact of numbers of antennas

Fig. 9 shows the effect of various numbers of antennas on the channel capacity and the capacity per antenna of a MIMO channel, respectively, when $d = \frac{\lambda}{2}$ and $K = -\infty$ dB, 4.77 dB, 6.99 dB. It is well known that MIMO channel capacity is proportional to the number of antennas [44–46]. From the figure, however, we note that the capacity will no longer linearly increase as the number of antennas increases. The total channel capacity increases slowly when the number of antennas exceeds about 20. Thus, it is not a good idea to increase the number of antennas without limit.

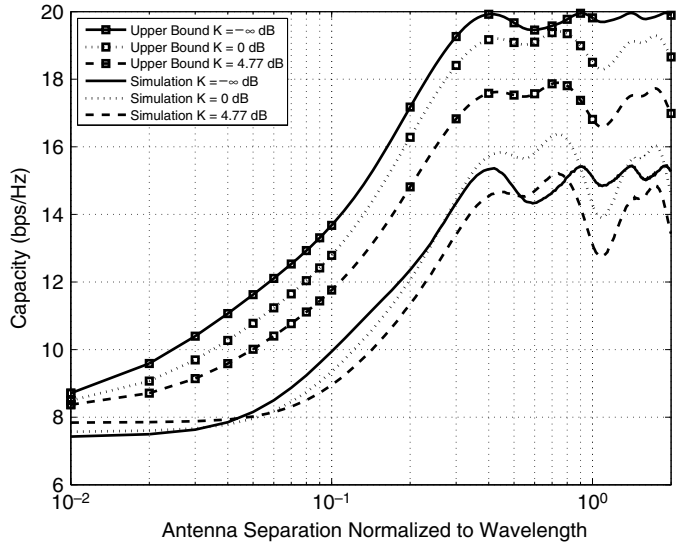

Fig. 8. Effect of antenna separation on the ergodic capacity of a 3×3 MIMO channel for SNR $= 20$ dB and various values of K factors.

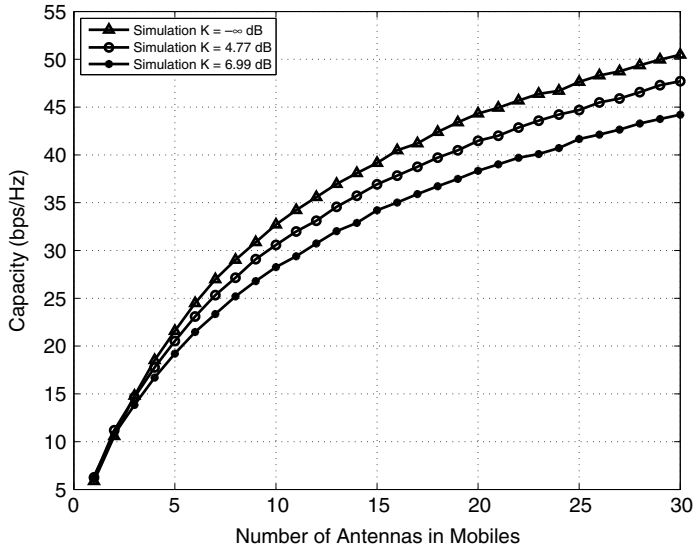

Fig. 9. The ergodic capacity of MIMO channels against the number of antennas when SNR $= 20$ dB, $d = \lambda/2$ and $I = N = 8$.

5.8. Impact of numbers of scatterers

Fig. 10 shows the effect of various numbers of scatterers on the total channel capacity of an MIMO system when $d = \frac{\lambda}{2}$ and $K = -\infty$ dB. We examine the effect of the number of scatterers on channel capacity with various numbers of scatterers (denoted by I and N). One can see that the total capacity is almost linearly proportional to the number of antennas when $I = N = 40$. When $I = N = 20$ and $I = N = 8$, due to less richness of the scatterers the total capacity of the MIMO channel is saturated as the number of antennas increases. Thus, if we want to obtain higher channel capacity by increasing the number of antennas, it is important to consider the scattering environment.

6. Conclusions

In this paper, we have developed a sum-of-sinusoids simulation method for the MIMO system in a mobile-to-mobile fading channel. Based on the double-ring scattering model with a LOS component [7], we incorporate the effect of Doppler effects, antenna separation, and LOS components for the MIMO system in a mobile-to-mobile environment. We have also derived the capacity upper bound of the mobile-to-mobile MIMO Rician channel. The channel capacity has been confirmed through simulations. We find that for MIMO systems with constant number of scatterers, increasing number of antennas cannot linearly increase the capacity. The capacity per antenna is decreased as Rician factor increases. We also find that the total channel capacity is related to the richness of the scattering environment. Besides, we proposed a "semi-analytical"

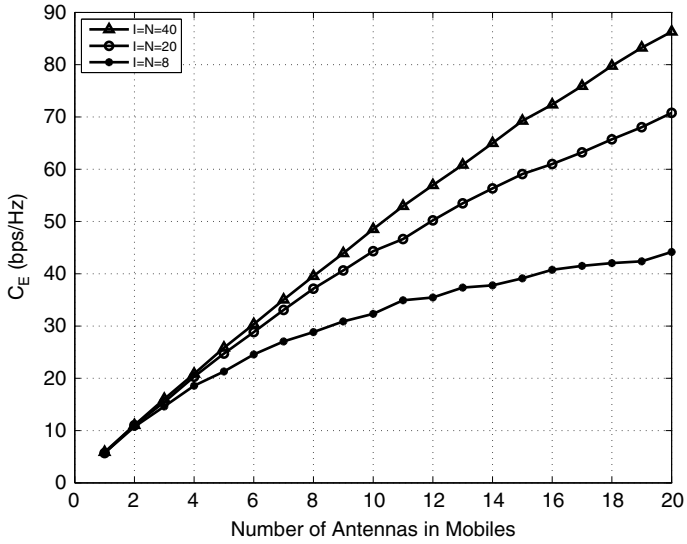

Fig. 10. The ergodic capacity of MIMO channels against the number of antennas for various numbers of scatterers (I and N) when SNR $= 20$ dB, $d = \lambda/2$ and $K = -\infty$ dB.

model for computing the LCR and AFD of the MIMO channel capacity. From those simulation results, we noted the influence of the LOS component, antenna separation, and number of scatterers on the MIMO channel capacity.

References

[1] J.-Z. Sun, J. Sauvola, D. Howie, Features in future: 4G visions from a technical perspective, in: Global Telecommunications Conference, 2001. GLOBECOM '01. IEEE, vol. 6, San Antonio, TX, USA, Nov. 25–29, 2001, pp. 3533–3537.
[2] IEEE P802.11—TASK GROUP N, Status of project IEEE 802.11n, Standard for enhancements for higher throughput. URL: http://www.ieee802.org/11/Reports/tgn_update.htm.
[3] P. Beckman, S. Verma, R. Rao, Use of mobile mesh networks for inter-vehicular communication, in: Vehicular Technology Conference, 2003. VTC 2003-Fall. 2003 IEEE 58th, vol. 4, Orlando, FL, USA, Oct. 6–9, 2003, pp. 2712–2715.
[4] S. Haykin, Cognitive radio: Brain-empowered wireless communications, IEEE J. Sel. Areas Commun. 23 (2005) 201–220.
[5] C.S. Patel, G.L. Stüber, T.G. Pratt, Simulation of Rayleigh faded mobile-to-mobile communication channels, in: Vehicular Technology Conference, 2003. VTC 2003-Fall. 2003 IEEE 58th, vol. 1, Orlando, FL, USA, Oct. 6–9, 2003, pp. 163–167.
[6] H. Kang, G.L. Stüber, T.G. Pratt, M.A. Ingram, Studies on the capacity of MIMO systems in mobile-to-mobile environment, in: Wireless Communications and Networking Conference, 2004. WCNC. 2004 IEEE, vol. 1, Atlanta, GA, USA, Mar. 21–25, 2004, pp. 363–368.
[7] L.-C. Wang, Y.-H. Cheng, A statistical mobile-to-mobile Rician fading channel model, in: Vehicular Technology Conference, 2005. VTC 2005-Spring. 2005 IEEE 61st, vol. 1, Stockholm, Sweden, May 30–Jun. 1, 2005, pp. 63–67.
[8] V. Erceg, L. Greenstein, S. Tjandra, S. Parkoff, A. Gupta, B. Kulic, A. Julius, R. Bianchi, An empirically based path loss model for wireless channels in suburban environments, IEEE J. Sel. Areas Commun. 17 (7) (1999) 1205–1211.
[9] V. Erceg, et al. Tgn channel models, document 03/940r4, IEEE 802.11 (May 10, 2004).
[10] Pekka Kyösti, et al. WINNER II channel models, deliverable d1.1.2 v1.2, Information Society Technologies (Sep. 30, 2007).
[11] 3GPP, 3rd generation partnership project; technical specification group radio access network; spatial channel model for multiple input multiple output (MIMO) simulations, 3GPP.
[12] M. Pätzold, B. Hogstad, N. Youssef, D. Kim, A MIMO mobile-to-mobile channel model: Part I — The reference model, in: Personal, Indoor and Mobile Radio Communications, 2005. PIMRC 2005. IEEE 16th International Symposium on, vol. 1, Berlin, Germany, Sept. 11–14, 2005, pp. 573–578.
[13] B. Hogstad, M. Pätzold, N. Youssef, D. Kim, A MIMO mobile-to-mobile channel model: Part II — The simulation model, in: Personal, Indoor and Mobile Radio Communications, 2005. PIMRC 2005. IEEE 16th International Symposium on, vol. 1, Berlin, Germany, Sept. 11–14, 2005, pp. 562–567.
[14] A. Zajič, G. Stüber, Space–time correlated MIMO mobile-to-mobile channels, in: Personal, Indoor and Mobile Radio Communications, 2006 IEEE 17th International Symposium on, Helsinki, Finland, Sept. 11–14, 2006, pp. 1–5.
[15] A. Zajič, G. Stüber, Simulation models for MIMO mobile-to-mobile channels, in: Military Communications Conference, 2006. MILCOM 2006. IEEE, Washington, DC, USA, Oct. 23–25, 2006, pp. 1–7.
[16] A. Zajič, G. Stüber, A three-dimensional MIMO mobile-to-mobile channel model, in: Wireless Communications and Networking Conference, 2007. WCNC 2007. IEEE, Hong Kong, China, Mar. 11–15, 2007, pp. 1883–1887.
[17] A. Zajič, G. Stüber, A three dimensional parametric model for wideband MIMO mobile-to-mobile channels, in: Global Telecommunications Conference, 2007. GLOBECOM '07. IEEE, Washington, DC, USA, Nov. 26–30, 2007, pp. 3760–3764.
[18] A. Chelli, M. Pätzold, A MIMO mobile-to-mobile channel model derived from a geometric street scattering model, in: Wireless Communication Systems, 2007. ISWCS 2007. 4th International Symposium on, Trondheim, Norway, Oct. 16–19, 2007, pp. 792–797.
[19] L.A.M. Guzman, A study on MIMO mobilte-to-mobile wireless fading channel models, Master's thesis, School of Engineering And Physical Sciences, Heriot Watt University (Jun. 2008), URL: http://www.amcomputersystems.com/vibot/vibots/mateos/index.html.
[20] A. Zajič, G. Stüber, Space–time correlated mobile-to-mobile channels: Modelling and simulation, IEEE Trans. Veh. Technol. 57 (2) (2008) 715–726.
[21] A. Zajič, G. Stüber, Three-dimensional modeling, simulation, and capacity analysis of space–time correlated mobile-to-mobile channels, IEEE Trans. Veh. Technol. 57 (4) (2008) 2042–2054.
[22] X. Cheng, C.-X. Wang, D. Laurenson, H.-H. Chen, A. Vasilakos, Space–time–frequency characterization of non-isotropic MIMO mobile-to-mobile multicarrier Ricean fading channels, in: Wireless Communications and Mobile Computing Conference, 2008. IWCMC '08. International, Crete Island, Greece, Aug. 6–8, 2008, pp. 994–999.
[23] X. Cheng, C.-X. Wang, D. Laurenson, H.-H. Chen, A. Vasilakos, A generic geometrical-based MIMO mobile-to-mobile channel model, in: Wireless Communications and Mobile Computing Conference, 2008. IWCMC '08. International, Crete Island, Greece, Aug. 6–8, 2008, pp. 1000–1005.
[24] A. Chelli, M. Pätzold, A wideband multiple-cluster MIMO mobile-to-mobile channel model based on the geometrical street model, in: Personal, Indoor and Mobile Radio Communications, 2008. PIMRC 2008. IEEE 19th International Symposium on, Cannes, France, Sep. 15–18, 2008, pp. 1–6.

[25] C. Wei, H. Zhiyi, X. Tao, Z. Wei, A novel isotropic scatter distribution wideband MIMO M2M fading channel model, in: Communication Networks and Services Research Conference, 2009. CNSR '09. Seventh Annual, Moncton, New Brunswick, Canada, May 11–13, 2009, pp. 443–445.
[26] J. Karedal, F. Tufvesson, N. Czink, A. Paier, C. Dumard, T. Zemen, C.F. Mecklenbräuker, A.F. Molisch, Measurement-based modeling of vehicle-to-vehicle MIMO channels, in: Communications, 2009. ICC '09. IEEE International Conference on, Dresden, Germany, Jun. 14–18, 2009.
[27] D. Gesbert, H. Bolcskei, D.A. Gore, A.J. Paulraj, Outdoor MIMO wireless channels: Models and performance prediction, IEEE Trans. Commun. 50 (2002) 1926–1934.
[28] A.F. Molisch, A generic model for MIMO wireless propagation channels in macro- and microcells, IEEE Trans. Signal Process. 52 (2004) 61–71.
[29] A. Giorgetti, P.J. Smith, M. Shafi, M. Chiani, MIMO capacity, level crossing rates and fades: The impact of spatial/temporal channel correlation, Int. J. of Commun. and Networks 5 (2003) 104–115 (special issue on coding and signal processing for MIMO systems).
[30] S. Wang, A. Abdi, J. Salo, H.M. El-Sallabi, J.W. Wallace, P. Vainikainen, M.A. Jensen, Time-varying MIMO channels: Parametric statistical modeling and experimental results, IEEE Trans. Veh. Technol. 56 (4) (2007) 1949–1963.
[31] D.-S. Shiu, G.J. Foschini, M.J. Gans, J.M. Kahn, Fading correlation and its effect on the capacity of multielement antenna systems, IEEE Trans. Commun. 48 (3) (2000) 502–513.
[32] D.-S. Shiu, Wireless Communication Using Dual Antenna Arrays, Kluwer Academic Publishers, Boston, Dordrecht, London, 2000.
[33] H. Shin, M.Z. Win, MIMO diversity in the presence of double scattering, IEEE Trans. Inform. Theory 54 (7) (2008) 2976–2996.
[34] W.C. Jakes, Microwave Mobile Communications, Wiley-IEEE Press, Piscataway, NJ, 1994.
[35] Y.R. Zheng, C. Xiao, Improved models for the generation of multiple uncorrelated Rayleigh fading waveforms, IEEE Commun. Lett. 6 (2002) 256–258.
[36] C. Xiao, Y.R. Zheng, A statistical simulation model for mobile radio fading channels, in: IEEE Wireless Commun. and Networking Conf., vol. 1, New Orleans, LA, USA, Mar. 16–20, 2003, pp. 144–149.
[37] A. Giorgetti, M. Chiani, M. Shafi, P. Smith, Level crossing rates and mimo capacity fades: Impacts of spatial/temporal channel correlation, in: Communications, 2003. ICC '03. IEEE International Conference on, vol. 5, Anchorage, AK, USA, May, 2003, pp. 3046–3050.
[38] P.-H. Kuo, P.J. Smith, Temporal behavior of MIMO channel quality metrics, in: Wireless Networks, Communications and Mobile Computing, 2005 International Conference on, vol. 2, Maui, HI, USA, Jun. 13–16, 2005, pp. 857–862.
[39] Wikipedia, Vehicular ad-hoc network, Wikipedia: The Free Encyclopedia, URL: http://en.wikipedia.org/wiki/VANET.
[40] D. Halliday, R. Resnick, Fundamentals of Physics, 3rd edition, John Wiley & Sons, New York, 1988.
[41] C. Xiao, Y.R. Zheng, N.C. Beaulieu, Second-order statistical properties of the WSS Jakes fading simulator, IEEE Trans. Commun. 50 (2002) 888–891.
[42] L.-C. Wang, Y.-H. Cheng, Modelling and capacity analysis of MIMO Rician fading channels for mobile-to-mobile communications, in: Vehicular Technology Conference, 2005. VTC-2005-Fall. 2005 IEEE 62nd, vol. 2, Dallas, TX, USA, Sep. 25–28, 2005, pp. 1279–1283.
[43] D. Tse, P. Viswanath, Fundamentals of Wireless Communication, Cambridge University Press, New York, 2005.
[44] A. Paulraj, R. Narbar, D. Gore, Introduction to Space–Time Wireless Communications, Cambridge University Press, 2003.
[45] G.J. Foschini, M.J. Gans, On limits of wireless communications in a fading environment when using multiple antennas, Wireless Personal Commun. 6 (1998) 311–335.
[46] I.E. Teletar, Capacity of multi-antenna Gaussian channels, AT&T Bell Lab. Tech. Memo.
[47] A. Papoulis, Probability, Random Variables, and Stochastic Process, 3rd edition, McGraw-Hill, 2001.
[48] P. Smith, M. Shafi, On a Gaussian approximation to the capacity of wireless MIMO systems, in: Communications, 2002. ICC 2002. IEEE International Conference on, vol. 1, New York City, NY, USA, Apr. 28–May 2, 2002, pp. 406–410.
[49] M. Shafi, P.J. Smith, An approximate capacity distribution for MIMO systems, IEEE Trans. Commun. 52 (2004) 887–890.
[50] C. Gao, M. Zhao, S. Zhou, Y. Yao, Capacity autocorrelation characteristic of MIMO systems over Doppler spread channels, in: Vehicular Technology Conference, 2003. VTC 2003-Spring. The 57th IEEE Semiannual, vol. 1, Jeju Island, Korea, Apr. 22-25, 2003, pp. 44–46.

Li-Chun Wang received the B.S. degree in electrical engineering from the National Chiao Tung University, Hsinchu, Taiwan, in 1986, the M.S. degree in electrical engineering from the National Taiwan University, Taipei, Taiwan, in 1988, and the M.Sc. and Ph.D. degrees in electrical engineering from Georgia Institute of Technology, Atlanta, in 1995 and 1996, respectively. From 1990 to 1992, he was with Chunghwa Telecom, Taoyuan, Taiwan. In 1995, he was with Northern Telecom, Richardson, TX. From 1996 to 2000, he was a Senior Technical Staff Member with the Wireless Communications Research Department, AT&T Laboratories. In August 2000, he became an Associate Professor with the Department of Communication Engineering, National Chiao Tung University, where he has been a Full Professor since August 2005. His research interests include cellular architectures, radio network resource management, and cross-layer optimization for cooperative and cognitive wireless networks. He is the holder of three U.S. patents and has three patents pending.

Dr. Wang is a corecipient of the Jack Neubauer Best Paper Award from the IEEE Vehicular Technology Society in 1997.

Wei-Cheng Liu received the B.S. and M.S. degrees in electrical engineering from the National Tsing Hua University, Hsinchu, Taiwan, in 1999 and 2001. He received the Ph.D. degree in Communications Engineering from the National Chiao Tung University, Hsinchu, Taiwan, in 2008.

He served the military service in Cheng Gong Ling, Taichung, Taiwan, from 2001 to 2002. In 2002, he was a GSM Layer-1 Software Engineer with Compal Communications, Taipei, Taiwan. He was a postdoctoral researcher in the Department of Communications Engineering, National Chiao Tung University, Hsinchu, Taiwan, from 2008 to 2009. In August 2009, he became an Assistant Professor with the Department of Communications Engineering, National Chung Cheng University. His research interests include MIMO Rician channels in mobile ad hoc networks, cross-layer rate and power adaptation for wireless LANs, performance analysis for UWB systems, space–time–frequency code design, and cooperative network coding.

Yun-Huai Cheng was born in Taiwan, R.O.C. in 1981. He received a B.Sc. in Electrical and Control Engineering from National Chiao Tung University, Hsinchu, Taiwan, in 2003, and the M.Sc. degree from the Department of Communication Engineering at National Chiao Tung University, Hsinchu, Taiwan, in 2005. His research interests are in the field of wireless communications and he is currently working in Foxconn International Holdings, Co., Ltd.